Cement & Concrete Composites 32 (2010) 62–72

Contents lists available at ScienceDirect

Cement & Concrete Composites

journal homepage: www.elsevier.com/locate/cemconcomp

Behavior of high performance fiber reinforced cement composites under multi-axial compressive loading

Kittinun Sirijaroonchai, Sherif El-Tawil *, Gustavo Parra-Montesinos

Dept. of Civil and Environmental Eng., University of Michigan, Ann Arbor, MI, United States

ARTICLE INFO

Article history:
Received 23 April 2009
Received in revised form 14 September 2009
Accepted 15 September 2009
Available online 19 September 2009

Keywords:
Strain hardening
Material properties
Multi-axial loading tests
Compressive behavior
Failure surface
Constitutive modeling

ABSTRACT

Experiments were conducted to better understand the behavior of strain hardening, high performance fiber reinforced cement composites (HPFRCC) when subjected to uniaxial, biaxial, and triaxial compression. The experimental parameters were: type of fiber, fiber volume fraction, and loading path. Two types of commercially available fibers, namely high-strength hooked steel fiber and ultra high molecular weight polyethylene fiber, with volume fractions ranging from 1.0% to 2.0%, were used in a 55-MPa mortar matrix. The selected loading paths consisted of uniaxial compression and tension, equal biaxial compression, and triaxial compression with two levels of lateral compression. The test results revealed that the inclusion of short fibers can significantly increase both strength and ductility under uniaxial and biaxial loading paths, but that the role of volume fraction is rather small for the range of fiber volume contents considered. The results also showed that the confining effect introduced by the fibers becomes minor in triaxial compression tests, where there is relatively high external confining pressure. The experimental information documented herein can serve as input for the development of multiaxial constitutive models for HPFRCCs.

1. Introduction

High performance fiber reinforced cement composites (HPFRCC) are a class of fiber cement composites that exhibit post-cracking strain hardening response when subjected to direct tension. While undergoing this hardening behavior, the composite experiences the formation of multiple cracks prior to damage localization (i.e. crack opening) [1]. The advantages of HPFRCCs include ductility, durability and high energy absorption capacity compared with normal concrete and conventional fiber reinforced concrete (FRC).

Fig. 1 shows a qualitatively comparison of the stress–strain response in tension of an unreinforced cement composite matrix, FRC and HPFRCC. It is clear from Fig. 1 that both the cement-based matrix and FRC soften once σ_{cc}, the composite cracking strength, is attained. In contrast, HPFRCCs exhibit a post-cracking hardening response up to a peak stress σ_{pc}, which typically occurs at strains of 0.5% or higher. These 'high performance' characteristics have heightened interest in using HPFRCC to achieve improved infrastructure durability and enhanced structural performance under extreme loading [2].

Motivated by the need to better understand and quantify material response, several studies in the literature have reported on the testing and characterization of both FRC and HPFRCC (e.g. [1–3]). These studies have focused, in particular, on understanding the uniaxial unconfined compressive and tensile responses of cementitious composites. In contrast, far fewer studies have addressed multi-axial response, perhaps because of difficulties associated with multiaxial testing of cementitious composites. Furthermore, most of these studies have focused on FRC and thus, the multi-axial response of HPFRCC is little known. In order to address this gap, which hinders the development of 3-D constitutive models for HPFRCC materials, a series of multiaxial material tests were undertaken. The main objective of these tests, which are reported in this paper, was to provide necessary experimental data for characterization of the multi-axial response of HPFRCCs.

2. Testing techniques for characterizing HPFRCC material response

Several tests, namely uniaxial, biaxial, and triaxial tests, must be performed in order to identify material parameters necessary to model the behavior of HPFRCC in three dimensions. Following is a succinct synopsis of these testing techniques, with particular emphasis on FRC and HPFRCC applications.

Since there is no standard test procedure for conducting a uniaxial tension test for FRC and HPFRCC, several issues must be taken into account when designing the test setup. These issues include the geometry and alignment of the specimen, and the boundary

* Corresponding author. Tel.: +1 734 764 5617; fax: +1 734 764 4292.
E-mail address: eltawil@umich.edu (S. El-Tawil).

0958-9465/$ - see front matter © 2009 Elsevier Ltd. All rights reserved.
doi:10.1016/j.cemconcomp.2009.09.003

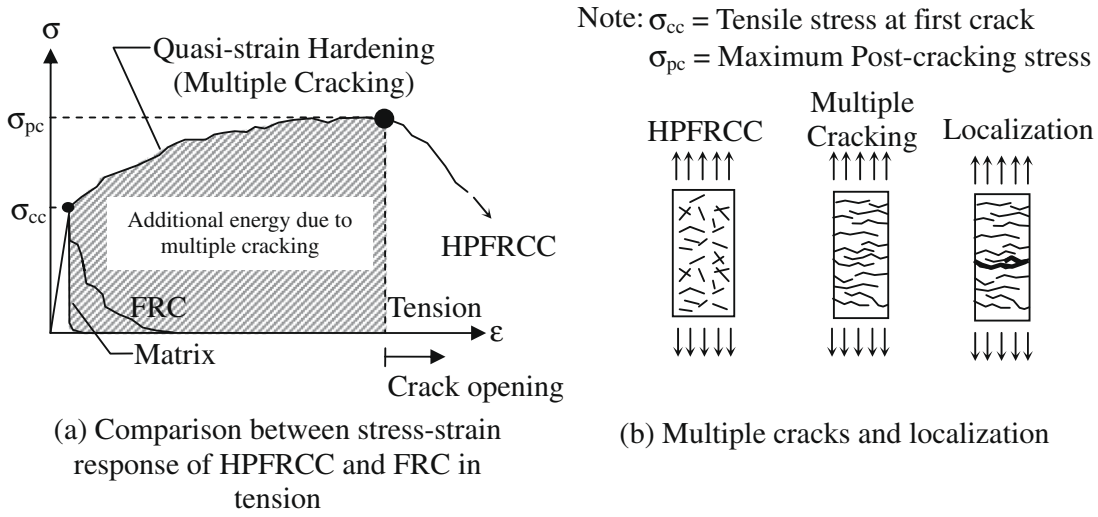

(a) Comparison between stress-strain response of HPFRCC and FRC in tension

(b) Multiple cracks and localization

Fig. 1. Typical stress–strain response in tension of high performance fiber reinforced cement composites (HPFRCC) [1].

conditions. In Ref. [3], it is shown that HPFRCC specimen size affects the strain value at the peak stress and that the difference in strain between small and large specimens could be as high as three times, with small specimens being more ductile than large specimens. When fixed loading platens are used, cracks that do not extend all the way across the specimen and uneven material properties can lead to eccentricities that create secondary flexural moments on the specimens. Partial width cracks are common in HPFRCC specimens because the material is ductile and non-homogeneous at the same time. Such partial cracks will cause redistribution of stress within a specimen and lead to higher fracture toughness than can be achieved with freely rotating boundary conditions [4].

The behavior of FRC under biaxial loading (compression–compression or tension–compression) has been studied using the same techniques as previously used to study the biaxial behavior of regular concrete. For example, Torrentti and Djebri [5] studied the behavior of FRC under biaxial loading conditions by using a test setup similar to that developed by Kupfer et al. [6], in which separate actuators are used to achieve a desired biaxial stress ratio. Demeke and Tegos [7] also used separate actuators to study the behavior of FRC under biaxial compression–tension. Instead of using separate actuators, Yin et al. [8] used a load bifurcation mechanism developed by Su and Hsu [9] to study the biaxial behavior of FRC. The main drawback of this loading scheme is that it limits the loading path that can be taken. Moreover, only compressive forces can be applied using this kind of loading mechanism.

The most common technique for conducting triaxial tests is the confined compression test. There are two variations for applying the confining pressure, namely active and passive confinement. In the former, the specimen is placed in a pressure cell filled with pressurized fluid [10]. Once the pre-defined confining pressure is reached, axial load is then applied and the axial stress–strain curve and lateral strain history are obtained. In specimens subjected to passive confinement, lateral pressure is

Table 1
Basic properties of hooked steel and spectra fibers.

Fiber type	Diameter (mm)	Length (mm)	Density (g/cc)	Tensile strength (MPa)	Elastic modulus (GPa)
Hooked	0.38	30	7.9	2300	200
Spectra	0.038	38	0.97	2585	117

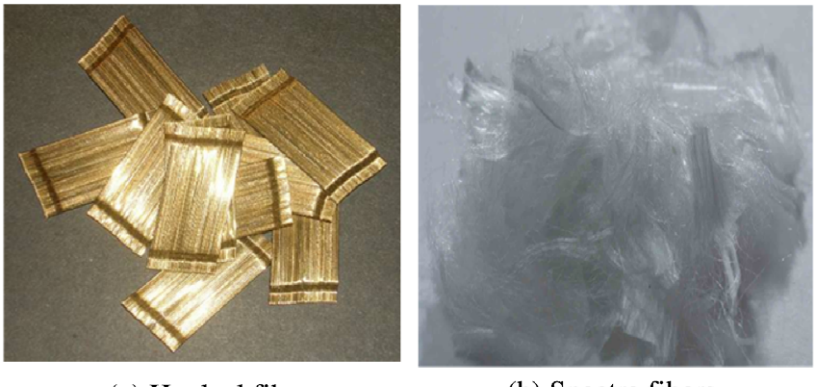

(a) Hooked fibers

(b) Spectra fibers

Fig. 2. Hooked steel fibers and spectra fibers.

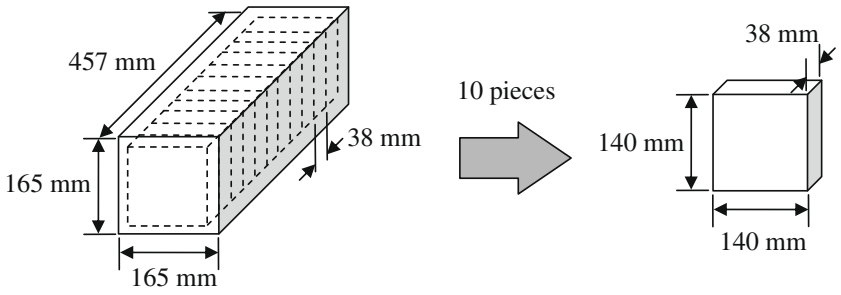

Fig. 3. Test panels obtained from slicing of a larger prism.

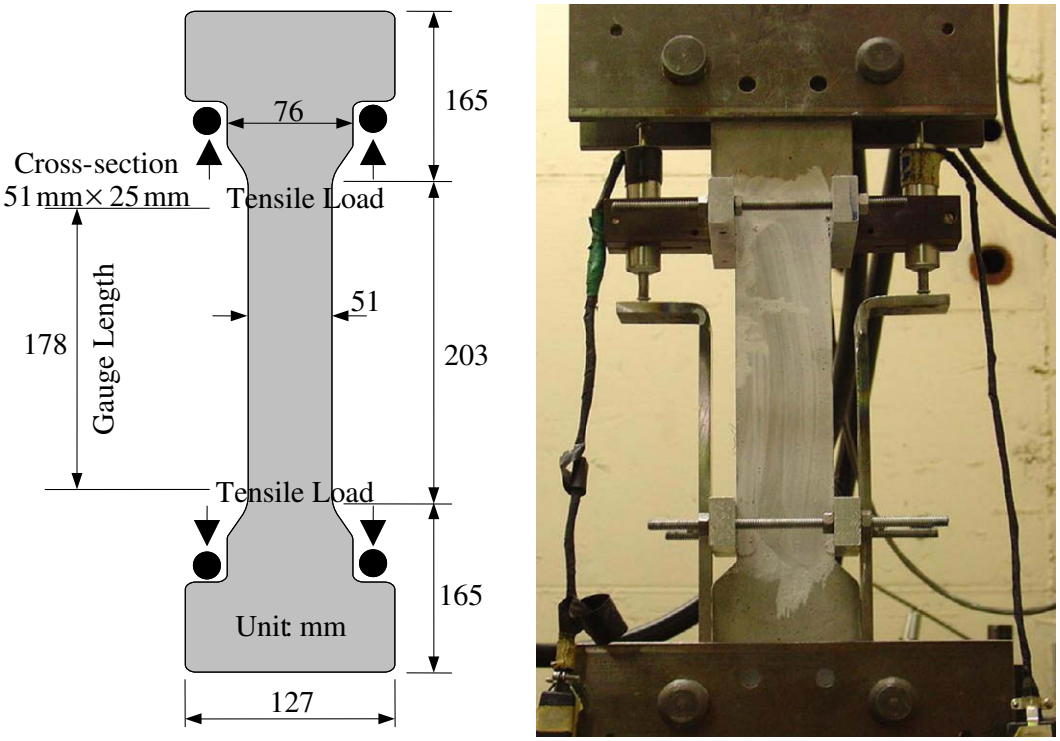

Fig. 4. Tension test specimen and setup.

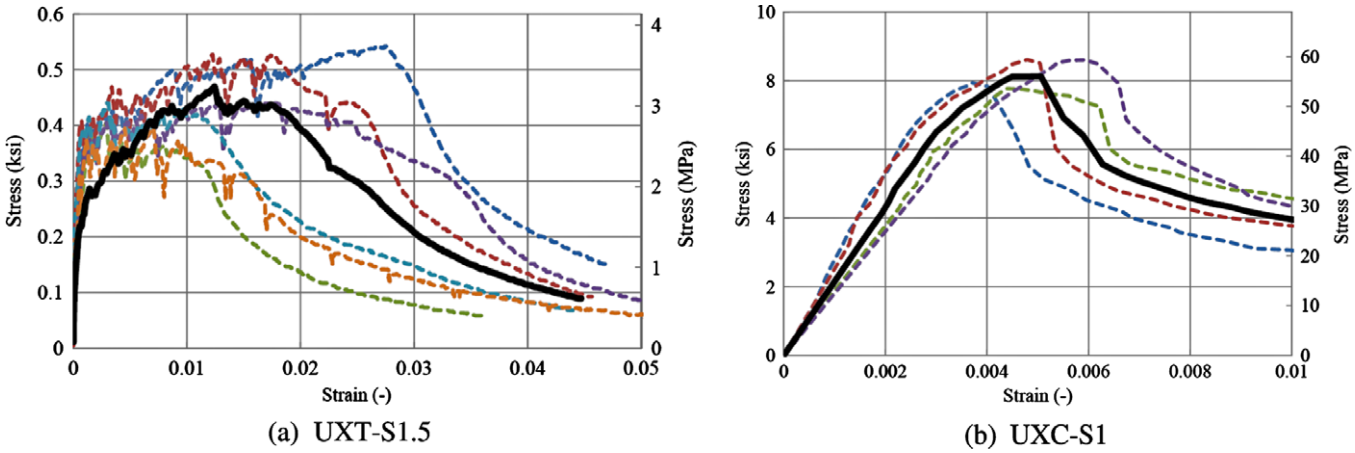

Fig. 5. Scatter in typical test series. Dotted lines represent individual test results while solid bold lines are the average of all test results in a series.

provided through transverse reinforcement (see for example Ref. [11]), typically in the form of either a steel or fiber reinforced polymer tube, or spiral or tie reinforcement. As axial load is applied, the concrete expands laterally due to the Poisson's effect, straining the transverse reinforcement, which translates into an increase in the confining pressure. Example of passive confining test setups using steel tubes can be found in [12] and [13], while some examples of test setups employing FRP wrapping are reported in [12] and [14].

3. Experimental program

3.1. Experimental parameters and specimen designation

The main experimental parameters in this study were fiber type, volume fraction and load path. Two types of fibers were used: (1) hooked (H) steel fiber, and (2) ultra-high molecular weight polyethylene fiber. The former is commercially available under the name of Dramix®, while the latter is found under the name

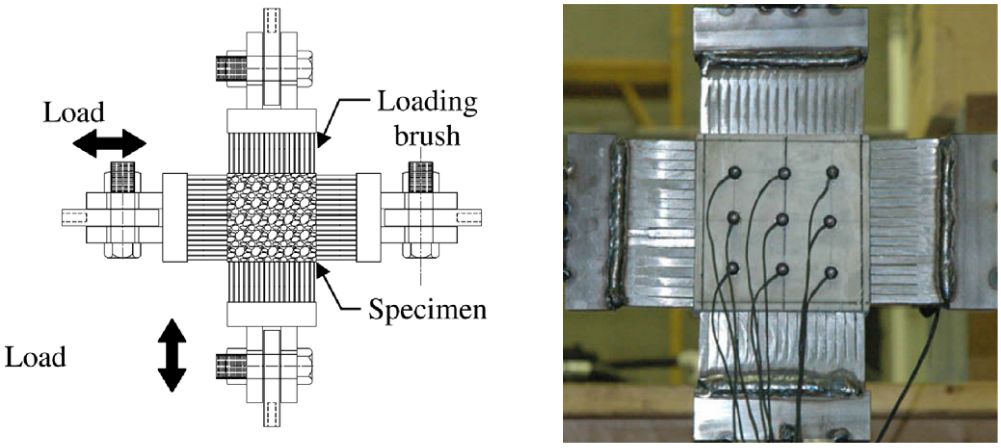

(a) Receivers to measure panel deformations (front panel)

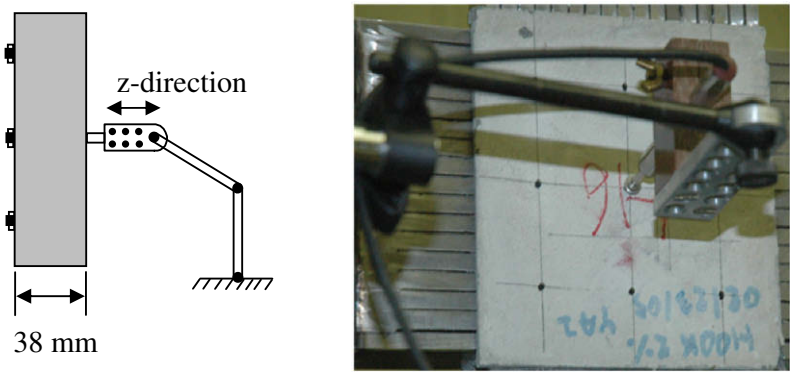

(b) LVDT attached to middle point of the back of the panel to measure out-of-plane expansion

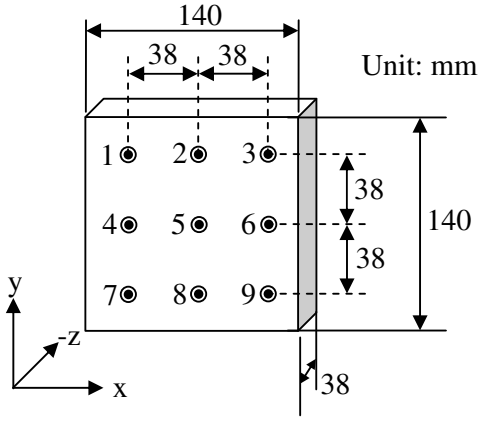

(c) Position of receivers on panel front

Fig. 6. Biaxial test setup with deformation measuring system.

spectra® (S). These fibers are shown in Fig. 2 and their properties listed in Table 1. These two fiber types were considered in three volume fractions, 1.0%, 1.5%, and 2.0%. The fibers were mixed with an approximately 55-MPa mortar with proportions by weight of 1:1:0.15: and 0.4 (cement type III: Flint sand with ASTM 30-70 gradation: fly ash class C: water).

To facilitate identification, each specimen is designated herein in a unique manner using a name comprised of three parts. The first term represents the loading conditions (UXCC for uniaxial compression of cylinder specimens; UXCR for uniaxial compression of square panel specimens; UXT for uniaxial tension; BXC for biaxial compression; TXC41 for triaxial compression with 41 MPa confining pressure; and TXC52 for triaxial compression with 52 MPa confining pressure). The second term in a specimen name represents the type of fibers (S for spectra; H for hooked; and M for unreinforced mortar). The third term represents fiber volume fraction (1%, 1.5%, and 2.0%). For example, UXCC-S1 stands for HPFRCC mixed with 1% spectra fibers for which a cylinder specimen is tested under uniaxial compression. TXC41-H1.5, on the other hand, stands for HPFRCC mixed with 1.5% hooked fiber tested under triaxial compression with 41 MPa confining pressure.

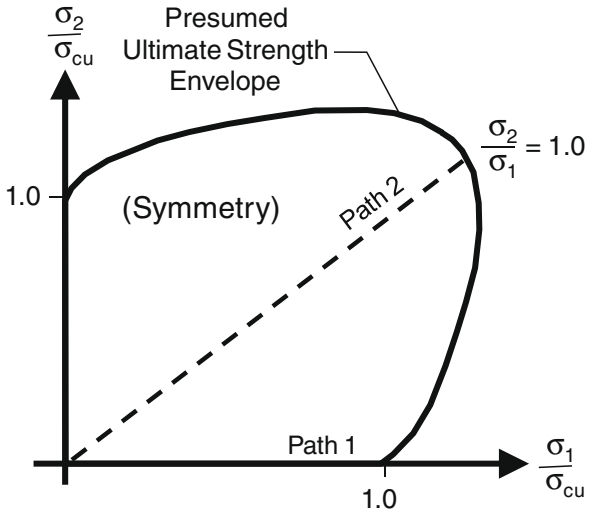

Fig. 7. Nominal loading paths in strain space under biaxial compression–compression loading.

3.2. Specimen production

Water was first pre-mixed with superplasticizer. All dry components (cement, sand, and fly ash) were mixed together in the mixing machine for a few minutes. Approximately half of the liquid part (i.e. water and superplasticizer) was then added to the dry mix. Once the dry components were fully mixed with the liquid part, fibers were slowly added in small amounts at a time while the rest of the liquid part was being intermittently added. Extra care was taken to prevent spectra fibers from clumping into balls. Once the mixing process was completed, the specimens (except for the triaxial test specimens) were cast into plastic molds placed on a shaking table in order to achieve good compaction. For the triaxial test specimens, the steel tube used to provide passive confinement served as the mold. Styrene foam cylinders with a thickness of 13 mm were placed at both ends of the steel tube to ensure that a clear depth was left on both ends. This allowed the application of the load directly to the HPFRCC material during the test.

After casting, the specimens were kept in their molds and covered with plastic sheets for approximately 24 h. They were then removed from the molds and placed in a water tank for curing for at least 28 days. In the case of the triaxial test specimens, the styrene foam cylinders were removed and the tube was fully submerged with the HPFRCC specimen. The specimens were then removed from the tank and left to dry 48 h prior to testing.

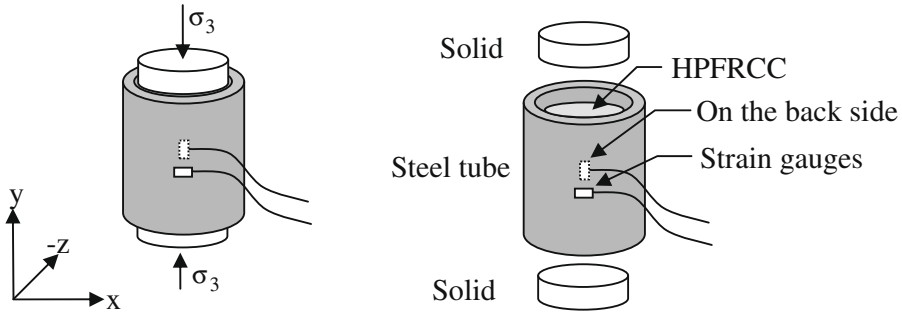

(a) Details of triaxial test specimen

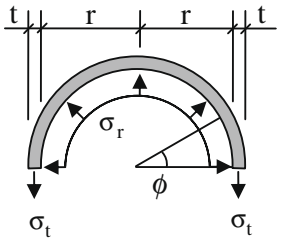

(b) Steel tube provides confining pressure [17]

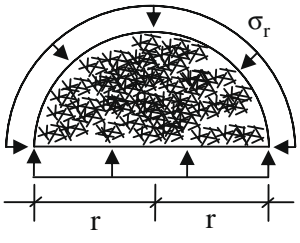

(c) Specimen subjected to confining pressure (modified from [17])

Fig. 8. Passive triaxial test setup.

Both ends of the uniaxial compression specimens were capped with a sulfur compound before testing to ensure an even loading surface. In order to avoid fiber alignment in the biaxial test due to their small thickness, a large prismatic specimen with dimensions 165 mm × 165 mm × 457 mm was first cast and then sliced into 10 specimens with the required size, as shown in Fig. 3.

3.3. Testing procedure

3.3.1. Tension tests

The uniaxial tension tests were performed on dog-bone shape specimens, as shown in Fig. 4. Two linear variable differential transformers (LVDTs) with gauge length of 178 mm were attached along the sides of the specimen in the loading direction. The tests were carried out in a universal testing machine at a stroke rate of 0.64 mm/min. A data acquisition system was used to record the applied load and LVDT readings. The deformation of the specimen was obtained by averaging the readings of the two LVDTs. To make sure that the test results were consistent, at least six tests were conducted for each series. Fig. 5a gives an idea of the statistical scatter observed in a typical tensile series.

3.3.2. Cylinder compression tests

Cylinder specimens with dimensions 76 mm × 152 mm were used for the uniaxial compression tests. Three LVDTs were attached along the side of the specimen to measure the longitudinal deformation up to the peak load. To prevent damage to the LVDTs from rapid deformation increases beyond the peak load, the LVDTs were removed and the post-peak deformation was obtained from the machine displacement instead. The full stress–strain response was then obtained by joining the two records. In the pre-peak regime, average strain was obtained by dividing the average of the three LVDT deformations by the LVDT gauge length. In the post-peak regime, average strain was obtained by dividing the machine deformation by the total specimen height. Average stress was directly obtained by dividing the machine load by the cross-sectional area of the cylinder. A minimum of three specimens within the same series were tested and average results are presented herein. Fig. 5b gives an idea of the statistical scatter observed in a typical compressive series.

3.3.3. Panel tests under uniaxial and biaxial compression tests

A total of thirty six 140 mm × 140 mm × 38 mm panel specimens were tested under biaxial loading using an existing test setup at the University of Illinois Newmark Structural Engineering Laboratory. This test setup consisted of four independent actuators, each with loading capacity of 500 kN. Each actuator was attached to the specimen sides with a brush-like platen (Fig. 6a) designed in such a way as to allow the specimen to freely expand in the transverse direction. The test setup was similar to that used by Kupfer et al. [6]. A non-contact displacement measurement system (Krypton®) was used for detailed measurement of the deformation in the test panels (Fig. 6a). The signal receivers were placed in the middle of the specimen, 38 mm apart from each other, as shown in Fig. 6c. In each direction, receivers were aligned into three lines and the two outer receivers were used to measure the in-plane deformation along each line. The deformation along each line was then converted to an average strain and the in-plane strain was obtained by averaging the three strains in each direction. Hence, the horizontal deformation was obtained by averaging the deformation of receivers 1–3, 4–6, and 7–9, whereas the vertical deformation was obtained by averaging the deformations of receivers 1–7, 2–8, and 3–9. In addition, an LVDT was attached to the back side of the specimen to measure, in combination with the receiver positions, the out-of-plane expansion (Fig. 6b). The out-of-plane deformation was obtained by adding the average z-deformation of all receivers to the deformation of the LVDT. Fig. 7 shows the load paths taken to investigate the biaxial

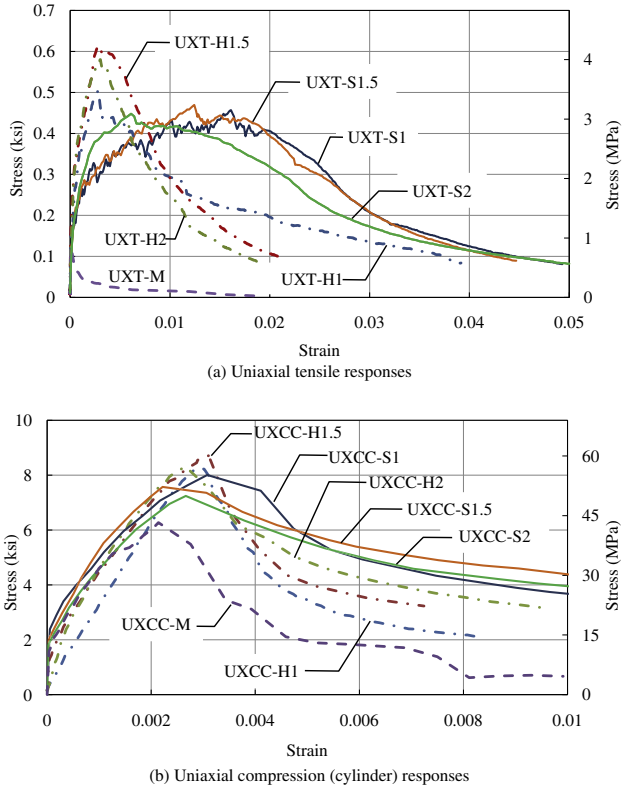

(a) Uniaxial tensile responses

(b) Uniaxial compression (cylinder) responses

Fig. 9. Uniaxial tensile and compressive responses of mortar and HPFRCC.

Table 2
Summary of key parameters describing uniaxial tension test results.

Fiber type	Fiber volume fraction (%)	ID	First crack		Peak strength	
			Stress (σ_{cc})[a] (MPa)	Strain (ε_{cc})[a] (%)	Stress (σ_{cc})[a] (MPa)	Strain (ε_{pc})[a] (%)
Spectra	1.0	UXT-S1	1.03	0.024	3.15	1.61
	1.5	UXT-S1.5	0.96	0.021	3.24	1.24
	2.0	UXT-S2	0.93	0.019	3.09	0.61
Hooked	1.0	UXT-H1	1.13	0.010	3.48	0.28
	1.5	UXT-H1.5	1.33	0.013	4.24	0.29
	2.0	UXT-H2	1.25	0.017	4.00	0.30
Mortar		UXT-M	0.82	0.013	–	–

[a] Refer to Fig. 1 for definition.

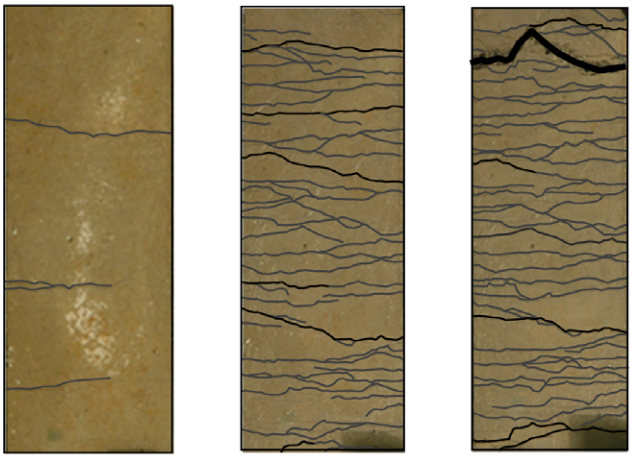

Fig. 10. Multiple cracks at different loading states in UXT-S1 specimen.

response of HPFRCC, i.e. Path 1 (denoted as UXCR) and Path 2 (denoted as BXC). Additional load paths were also investigated to fully characterize the failure surface, but those results will be presented in a forthcoming publication.

3.3.4. Triaxial tests

Passive triaxial tests were performed using a 2200 kN compression machine. A steel tube, 76 mm in nominal diameter and 178 mm in height, was used to encase the HPFRCC specimens to produce the necessary confinement (Fig. 8). The level of passive confinement was varied by changing the thickness of the tube as discussed next. Three LVDTs were placed along the side of the tube for measuring longitudinal deformation and two strain gauges were attached to the tube at the mid-height (on opposite sides of the tube) in both longitudinal and circumferential directions. The longitudinal strain gauges were used to evaluate the effect of friction between the specimen and the tube, which turned out to have a minor effect. The circumferential strain gauges were used to measure the expansion of the tube, which was then converted to confining pressure.

Dog-bone shaped steel pieces were cut from the tube and direct tension tests were performed to obtain the stress–strain curves of the steel tube, which were then used to convert the circumferential strain to stress. This stress was then converted to confining pressure using the following expression:

$$\sigma_r = \frac{\sigma_t t}{r} \quad (1)$$

where σ_r is the confining pressure, σ_t is the circumferential stress, r and t are the radius and and thickness of steel tube, respectively. The two tube thicknesses used in this study were 1.6 and 3.2 mm, which corresponded to confining pressures at steel tube yielding of 41 and 52 MPa, respectively.

4. Discussion of experimental results

4.1. Uniaxial tensile response

The uniaxial tensile stress–strain responses of mortar and HPFRCC specimens are shown in Fig. 9a and summarized in Table 2. Clearly, the response of plain mortar (UXT-M) was brittle under tension, i.e. linear elastic up to the first crack, followed by an abrupt drop in stress. The addition of fibers changed the response dramatically and eliminated damage localization after first

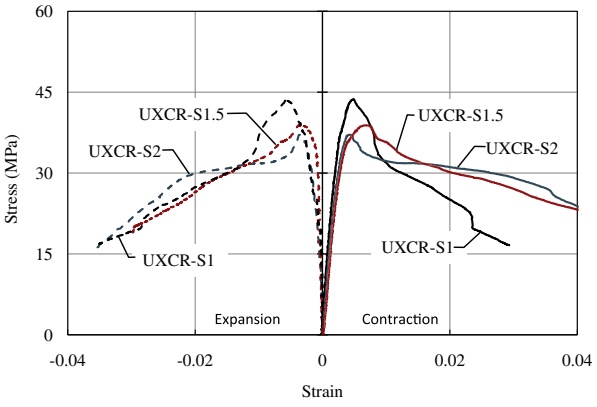

(a) Specimens with Spectra fibers

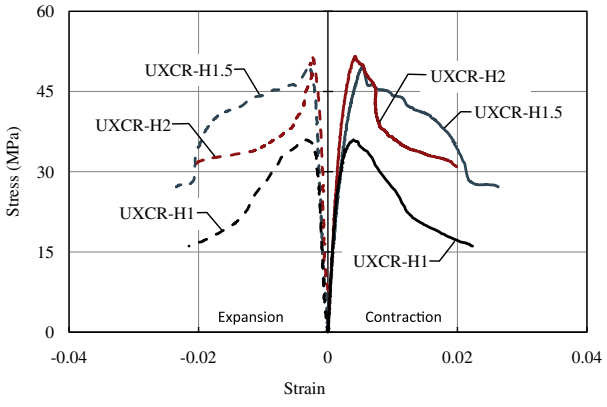

(b) Specimens with hooked fibers

Fig. 11. Uniaxial compressive responses of HPFRCC panels.

Table 3
Summary of key parameters describing compression cylinder test results.

Fiber type	Fiber volume fraction (%)	ID	Young's modulus (GPa)	Peak point		Post-peak strain at 40% of f'_c (%)
				Strength (f'_c) (MPa)	Strain (%)	
Spectra	1.0	UXCC-S1	37.4	55.2	0.31	1.23
	1.5	UXCC-S1.5	45.0	52.2	0.22	1.79
	2.0	UXCC-S2	29.6	49.9	0.27	1.88
Hooked	1.0	UXCC-H1	21.3	56.9	0.29	0.52
	1.5	UXCC-H1.5	37.0	60.3	0.31	0.62
	2.0	UXCC-H2	36.5	57.2	0.26	0.85
Mortar		UXCC-M	26.6	43.3	0.21	0.43

cracking. For the range of fiber volume fraction considered (between 1% and 2%), fiber content played a relatively small role in specimen response.

All specimens mixed with either type of fibers (UXT-H and UXT-S) showed strain-hardening behavior along with multiple cracking (Fig. 10). Other enhancements were evident too. On average, the strength of all UXT-H series was about five times that of plain mortar. Similarly, the strength of the UXT-S specimens was approximately four times higher than the average strength of plain mortar. In term of ductility, the specimens with spectra fibers (UXT-S) showed greater ductility than those with hooked steel fibers (UXT-H). Specifically, at 2% strain, the UXT-S specimens were able to maintain a stress level of approximately three-quarters of the tensile strength, whereas the UXT-H specimens sustained only a quarter of the peak stress (Fig. 9a).

4.2. Uniaxial compressive response

The uniaxial compressive stress–strain responses of the mortar and HPFRCC specimens are shown in Fig. 9b and summarized in Table 3. The peak strength and corresponding strain in the HPFRCC specimens was clearly greater that those in the mortar specimens. Specifically, the average peak strength of the cylinders with hooked steel fibers (UXCC-H) for all volume was increased by approximately 25%, regardless of the fiber content, whereas the corresponding average strain at peak stress increased by approximately 50% over the corresponding mortar values. In terms of post-peak response, a more gradual decrease in stress and an increase in strain capacity were observed on the HPFRCC specimens. The enhancements in strength, peak strain and ductility can be attributed to the fact that the dispersed fibers hindered lateral expansion, which in turn increased the confining pressure. Since mortar is a pressure dependent material, increasing confining pressure enhanced both the strength and the ductility of the material. As with the tensile test results, the role of fiber volume fraction was not large for the fiber content range considered (1–2%).

The uniaxial compressive responses obtained from the biaxial test setup (Path 1 in Fig. 7, denoted as UXCR) are shown in Fig. 11, where the longitudinal stress is plotted against both longi-

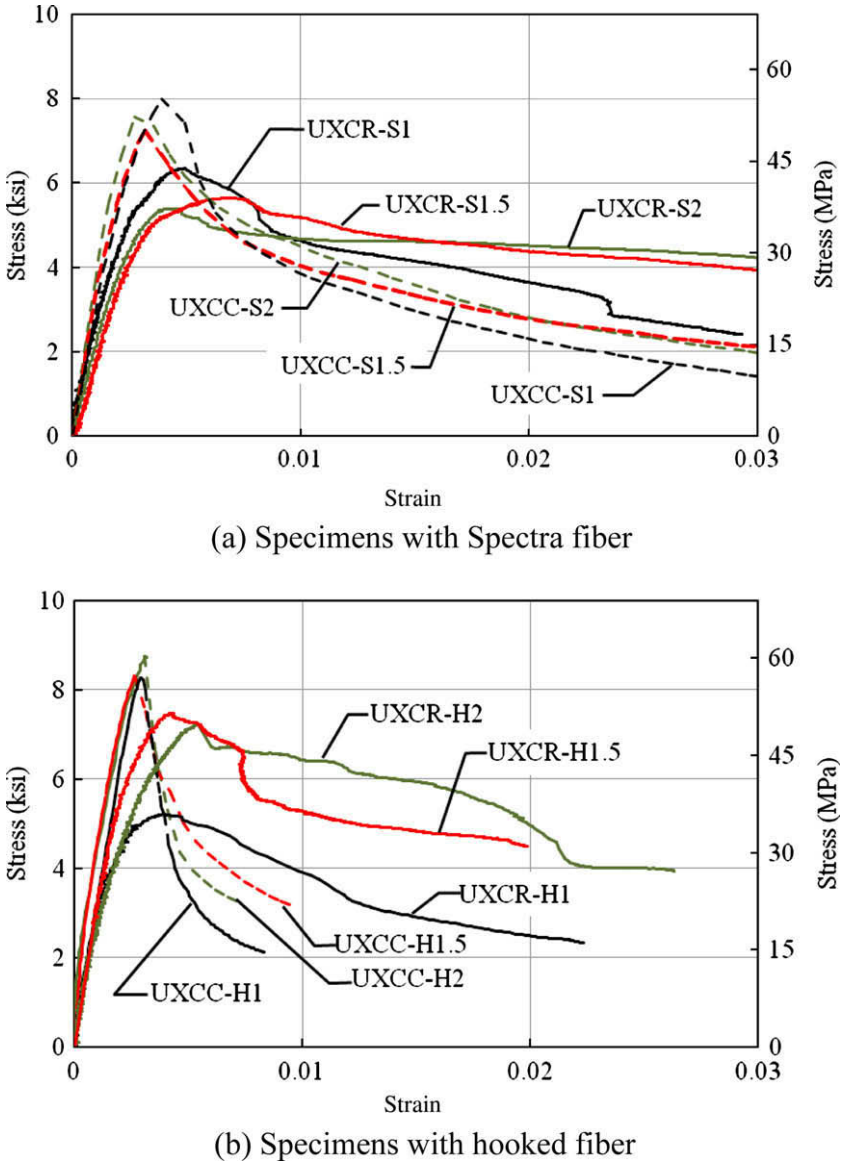

Fig. 12. Comparison of uniaxial compressive response of cylindrical and panel specimens.

tudinal and transverse strains. The uniaxial responses obtained from panel specimens with rectangular cross-section are also compared to those from traditional cylindrical specimens (Fig. 12). Key observations from Fig. 12 are: (1) Young's moduli obtained from both test setups were almost identical; (2) cylindrical specimens gave higher compressive strength than panel specimens; (3) cylindrical specimens appeared to be less sensitive to the fiber content than the panel specimens.

Another observation from Fig. 12 is that the post-peak response drops off more sharply in the cylindrical specimens compared to the panel ones, particularly for specimens reinforced with hooked steel fibers (Fig. 12b). It is believed that the main reason for this difference lies in fiber distribution. The narrowness of the cylindrical specimens may have caused some directionality in fiber orientation compared to the larger prism from which the panel specimens were cut, which would have reduced the efficiency of fiber reinforcement to control lateral expansion in the cylinder specimens.

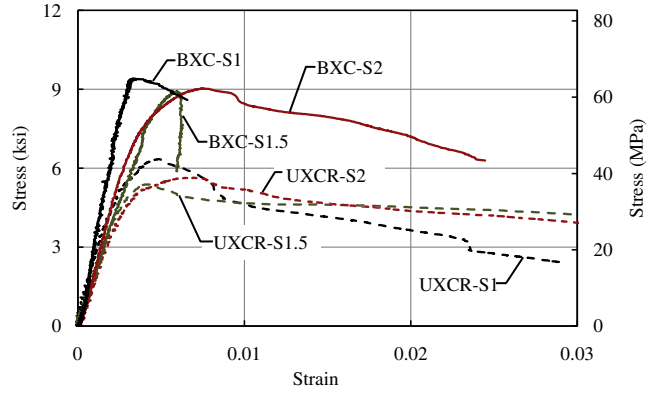

(a) Specimens with Spectra fiber

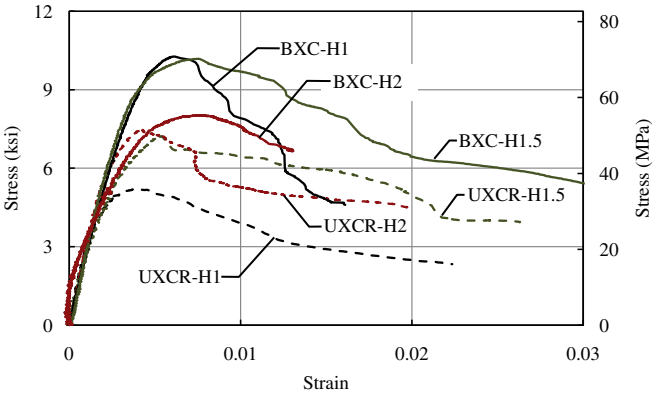

(b) Specimens with hooked fiber

Fig. 13. Comparison of uniaxial compression and equal biaxial compression responses.

4.3. Biaxial compressive responses

The equal biaxial compressive responses are compared to the corresponding uniaxial compressive responses in Fig. 13. In the pre-peak regime, the initial slopes of both uniaxial and equal biaxial compression specimens were nearly identical for corresponding specimens for both types of fibers. However, there was a clear improvement in compressive strength under biaxial loading compared to uniaxial loading. Except for specimens BXC-S1 and BXC-S1.5, where some of the receivers detached prematurely preventing complete processing of the results, the post-peak responses of corresponding uniaxial and biaxial specimens appear to be similar. Plain mortar specimens were not tested because they tended to fail explosively and were deemed a safety concern.

Table 4 summarizes the key parameters of the peak point of HPFRCC specimens under uniaxial and equal biaxial compression. Under equal biaxial compression (BXC), the ratio between the peak strength and the unconfined compressive strength is 1.5 and 1.6 in HPFRCC constructed with hooked and spectra fibers, respectively. This is in contrast to 1.1 and 1.2 for high strength and normal concrete, respectively, as noted in [15]. The strength enhancement of HPFRCC over regular concrete is attributed to the presence of fibers, which provided confinement, reducing out-of-plane expansion, and increasing compressive strength compared to regular concrete.

4.4. Triaxial compressive response

The stress–strain responses of HPFRCC under triaxial compression test are plotted in Fig. 14, while Table 5 summarizes key parameters describing the triaxial response of all series tested. Two key observations from Fig. 14 and Table 5 are that: (1) the peak strength (f_{max} in Table 5) was approximately the same in all series for the same level of confinement; and (2) the overall stress–strain response was not influenced by the type or volume fraction of fibers used. Both observations are believed to be a consequence of the heavy confinement provided by the steel tube, which overshadowed the effect of the fibers.

Fig. 15 illustrates the response of the triaxial test series with 2% volume fraction of spectra fibers under all compressive loading conditions considered in this study. A key observation that can be exploited in the development of a constitutive model is that the initial slope of the responses under all loading conditions is approximately equal, i.e. Young's modulus is not influenced by the loading condition. On the other hand, and as previously pointed out, it is clear that strength and ductility are improved as the level of external confining pressure increases.

5. Summary and conclusions

The behavior of fiber reinforced cement composites under uniaxial, biaxial, and triaxial stress states was experimentally evaluated.

Table 4
Summary of key parameters describing biaxial compression test results.

Fiber type	Fiber volume fraction (%)	Peak point							
		Uniaxial compression				Compression–compression			
		Horizontal		Vertical		Horizontal		Vertical	
		Stress (MPa)	Strain (%)	Stress (MPa)	Strain (%)	Stress (MPa)	Strain (%)	Stress (MPa)	Strain (%)
Spectra	1.0	–	−0.53	43.8	0.53	65.0	0.28	64.5	0.49
	1.5	–	−0.31	37.2	0.43	59.4	0.68	68.8	0.64
	2.0	–	−0.36	38.9	0.68	66.0	0.71	57.9	0.93
Hooked	1.0	–	−0.37	36.1	0.44	68.8	0.58	71.5	0.70
	1.5	–	−0.29	49.9	0.56	69. 3	0.53	70.6	0.70
	2.0	–	−0.42	51.6	0.72	64.8	0.81	65.8	0.73

Note: Negative strain represents expansion.

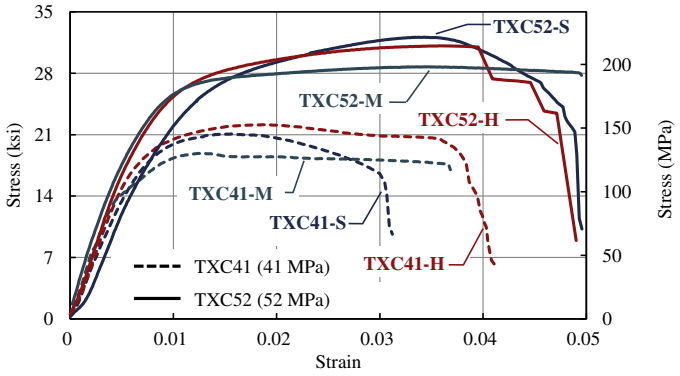

Fig. 14. Triaxial compressive response of HPFRCC.

Table 5
Summary of key parameters describing triaxial compression test results.

Type of fiber	Fiber volume fraction (%)	Confining pressure					
		41 MPa			52 MPa		
		f_{max} (MPa)	ε_{max} (%)	$\varepsilon_{v,min}$ (%)	f_{max} (MPa)	ε_{max} (%)	$\varepsilon_{v,min}$ (%)
Spectra	1.0	146	2.50	−0.53	222	3.70	−0. 91
	1.5	148	4.00	−0.61	225	4.20	−0. 71
	2.0	141	4.50	−0.61	218	4.80	−0. 92
Hooked	1.0	148	1.50	−0.55	215	3.30	−0. 54
	1.5	152	2.20	−0.55	215	4.00	−0. 40
	2.0	157	1.80	−0.59	222	4.10	−0. 43
Mortar		130	1.30	−0.33	198	3.40	−0. 71

f_{max}: Maximum stress.
ε_{max}: Longitudinal strain at maximum stress (positive number represents contraction).
$\varepsilon_{v,min}$: Minimum volumetric strain (negative number represents contraction).

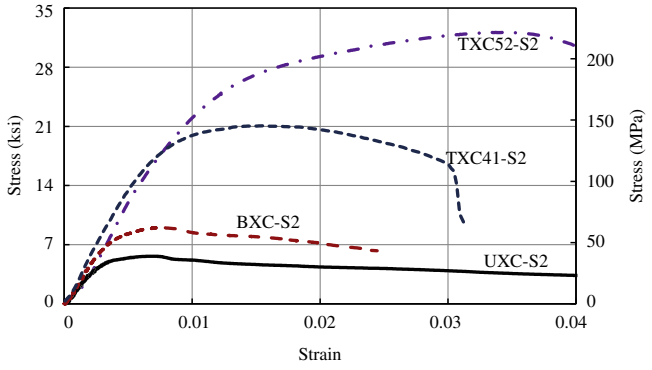

Fig. 15. Comparison of stress–strain responses of HPFRCC under various compressive loading conditions.

Two types of fibers, namely hooked steel fiber and ultra high molecular weight polyethylene (spectra) fiber, were evaluated at three different volume fractions (1%, 1.5%, and 2%). The fibers were mixed with a mortar with a target compressive strength of 55 MPa. The following conclusions can be drawn from the limited test results:

- Under uniaxial tension, strain-hardening behavior, accompanied with multiple cracking, was achieved in all specimens mixed with either type of fibers. Tensile strength was significantly improved compared with unreinforced mortar. For example, the average strength of specimens with hooked steel fibers was approximately five times that of plain mortar, while the specimens with spectra fibers exhibited about four times the strength of plain mortar. Ductility also increased significantly, although specimens with spectra fibers were, in general, more ductile than those with hooked steel fibers.
- Under uniaxial compression, the inclusion of fibers had little effect on the pre-peak response, but significant effect on the peak and post-peak responses. For example, the average peak strength of the specimens with hooked steel fibers increased by approximately 25%, whereas the corresponding average strain at peak increased by about 50% over the corresponding mortar values. Both the strength enhancement and the pronounced gradual softening behavior were attributed to the fibers hindering lateral expansion, which in turn increased the confining pressure thereby improving performance.

- The strength ratio between equal biaxial and uniaxial compression was significantly greater for composites with hooked and spectra fibers (1.5 and 1.6, respectively) compared to that of plain concrete (1.1 and 1.2 for high-strength and normal strength concrete, respectively). The enhancement was attributed to the presence of fibers, which reduced out-of-plane expansion, improving confinement and thus increasing compressive strength.
- Under triaxial compression, the overall stress–strain response was not significantly influenced by the presence of either type of fibers. This was attributed to the heavy confinement provided by the steel tube, which is significantly larger than the confining effect introduced by the fibers.
- For the range of fiber volume fraction considered (between 1% and 2%), the role of fiber content in the compression and tension behavior of the test specimens was found to be rather small.
- The tests results reported in this paper provide a detailed picture of the response of HPFRCCs subjected to various 3-D load paths, which is necessary information for formulating and calibrating multiaxial constitutive models for HPFRCCs. The data presented, however, only pertains to monotonic loading. Additional research is needed to study the multi-axial response of HPFRCC under cyclic loading.

Acknowledgements

This research was sponsored in part by the US National Science Foundation under Grants No. CMS 0530383 and 0754505 and the University of Michigan. Prof. James LaFave and his students Adrianne Wheeler and Ray Foltz of the University of Illinois at Urbana-Champaign helped conduct the biaxial tests. The authors acknowledge and are grateful for the ideas, help and expertise of Prof. Antoine E. Naaman at the University of Michigan. The opinions, findings, and conclusions expressed in this paper are those of the authors alone and do not necessarily reflect the views of the sponsors or the individuals mentioned here.

References

[1] Naaman A E, Reinhardt H W. Characterization of high performance fiber reinforced cement composites – HPFRCC. In: Naaman AE, Reinhardt HW, editor. High performance fiber reinforced cement composites, vol. 2. Ann Arbor; 1996. p. 1–24.
[2] Kim DJ, Naaman AE, El-Tawil S. Comparative flexural behavior of four fiber reinforced cementitious composites. Cem Concr Compos 2008;30:917–28.
[3] Chandrangsu K. Innovative bridge deck with reduced reinforcement and strain-hardening fiber reinforced cementitious composites. Ph.D. Dissertation, University of Michigan, Ann Arbor; 2003.
[4] Van Mier JGM, Van Vliet MRA. Uniaxial tension test for the determination of fracture parameters of concrete: state of the art. Eng Fract Mech 2002;69(2):235–47.
[5] Torrentti JM, Djebri B. Behavior of steel-fiber-reinforced concretes under biaxial compression loads. Cem Concr Compos 1995;17:261–6.
[6] Kupfer H, Hilsdorf HK, Rusch H. Behavior of concrete under biaxial stresses. ACI J 1969;66(8):656–66.
[7] Demeke A, Tegos IA. Steel fiber reinforced concrete in biaxial stress tension–compression conditions. ACI Mater J 1994;91(5):579–84.
[8] Yin WS, Su ECM, Mansur MA, Hsu TTC. Fiber-reinforced concrete under biaxial compression. Eng Fract Mech 1990;35:261–8.
[9] Su ECM, Hsu TTC. Biaxial compression fatigue and discontinuity of concrete. ACI Mater J 1988;85(3):178–88.
[10] Richart FE, Brandtzaeg A, Brown RL. A Study of the failure of concrete under combined compressive stresses. University of Illinois Bulletin; 1928 [vol. 26(12)].
[11] Roy HEH, Sozen MA. A model to simulate the response of concrete to multiaxial loading. Structural research series No. 268. University of Illinois; 1963 [June].
[12] Pantazopoulou SJ, Zanganeh M. Triaxial tests of fiber-reinforced concrete. J Mater Civ Eng 2001;13(5):340–8.
[13] Ahmad SH, Shah SP. Complete triaxial stress–strain curves for concrete. ASCE J Struct Div 1982;108(ST4):728–42.
[14] Spoelstra MR, Monti G. FRP-confined concrete model. J Compos Construct 1999;3(3):143–50.
[15] Hussein A, Marzouk H. Behavior of high-strength concrete under biaxial stresses. ACI Mater J 2000;97(1):27–36.